International Journal of Rheumatic Diseases

WILEY

International Journal of Rheumatic Diseases

ORIGINAL ARTICLE OPEN ACCESS

The Role of Abatacept on Inflammation and Fibrosis in Hypochlorous Acid-Induced Fibrosis Mice

Bingying Dai[1] | Meng Meng[2] | Weilin Chen[1] | Junyu Zhou[1] | Qiming Meng[1] | Liqing Ding[1] | Shasha Xie[1] | Ding Bao[1] | Xiaojing Li[1] | Lijuan Zhao[1] | Ting Huang[1] | Chunliu Lv[3] | Hui Luo[1,4,5] | Sijia Liu[1,4,5] | Honglin Zhu[1,4,5]

[1]The Department of Rheumatology and Immunology, Xiangya Hospital of Central South University, Changsha, People's Republic of China | [2]Department of Pathology, Xiangya Hospital, Changsha, People's Republic of China | [3]Department of Breast Tumor Plastic Surgery, Hunan Cancer Hospital and the Affiliated Cancer Hospital of Xiangya School of Medicine, Central South University, Changsha, People's Republic of China | [4]Provincial Clinical Research Center for Rheumatic and Immunologic Diseases, Xiangya Hospital, Changsha, People's Republic of China | [5]National Clinical Research Center for Geriatric Disorders, Xiangya Hospital, Changsha, People's Republic of China

Correspondence: Sijia Liu (celialiu@csu.edu.cn) | Honglin Zhu (honglinzhu@csu.edu.cn)

Received: 1 November 2024 | **Revised:** 17 April 2025 | **Accepted:** 22 April 2025

Funding: This work was supported by the Natural Science Foundation of Hunan Province and the National Natural Science Foundation of China.

Keywords: abatacept | HCLO-induced fibrosis model | immune infiltration | RNA-seq | systemic sclerosis

ABSTRACT

Aim: To investigate the effect of abatacept in the hypochlorous acid (HCLO)-induced fibrosis model and to analyze changes in immune cell fractions within the abatacept-treated early diffuse systemic sclerosis (SSc) cohort.

Methods: Fibrosis was induced in BALB/c mice by subcutaneous injection of HCLO, and abatacept was injected intraperitoneally on alternate days starting on day 28. After 6 weeks, we assessed the pathological changes, inflammation, myofibroblast activation, and the percentage of ICOS in CD3+ T cells. Potential pathways affected by abatacept were also investigated. Finally, we analyzed immune infiltration and multiple scores in early diffuse SSc patients and in the skin and lung tissues of the HCLO model after abatacept administration.

Results: Abatacept significantly decreased the proportion of M2 macrophages in the abatacept-treated HCLO model and the inflammatory improver subset of SSc patients. Furthermore, abatacept reduced CD28 signaling, the inflammation-related pathway, and the ICOS expression on CD3+ T cells in HCLO mice. In the inflammatory subset of SSc patients and HCLO mice, microenvironmental and immune scores tended to decrease after abatacept treatment. Unexpectedly, abatacept had no effect on skin or lung collagen content in HCLO mice. The number of T cells and myofibroblasts was not reduced in the abatacept-treated HCLO group.

Conclusion: Although abatacept did not improve skin and lung fibrosis in the HCLO mice, it reduced the immune response signature and the proportion of M2 macrophages. These findings suggest that further research is needed to assess the therapeutic value of abatacept in SSc patients and preclinical mouse models.

1 | Introduction

Systemic sclerosis (SSc) is a systemic autoimmune disease of unknown etiology characterized by microvascular disease, abnormal autoimmune response, and progressive fibrosis [1–3]. Dysregulation of both immunity and inflammation plays a prominent part in SSc. The activated immune cells have been highlighted in the early stages of the disease [4–7]. Therefore, the activation of fibroblasts and the deposition of extracellular matrix (ECM) in the skin and visceral organs

place a significant burden on the later stages of SSc patients. Pulmonary fibrosis is the primary cause of mortality among SSc patients, and there is presently no cure for its treatment [8, 9].

Dysregulated T-cell activation is thought to have a substantial impact on the pathogenesis of SSc disease [4]. Co-stimulation, which CD28 mediates, is fundamental in facilitating T-cell activation and function [10]. Blocking this pathway demonstrates potential in treating aberrant autoimmune diseases. CTLA-4 is an effective inhibitor of the costimulatory interactions of CD28-B7 by binding with high affinity to CD80 and CD86 [11–13]. Consequently, it acts as an antagonist to this pathway.

Abatacept, a CTLA-4-Ig fusion protein, has been approved to restrain the adaptive immune response and downregulate a series of pro-inflammatory agents, such as interleukin (IL)-6, tumor necrosis factor (TNF)-α, IL-1β, and transforming growth factor (TGF)-β [14, 15]. In a preliminary observational study of 11 SSc patients, EUSTAR showed that abatacept improved skin and musculoskeletal activity after 24 months of drug monitoring in juvenile localized scleroderma (jLS) patients resistant to standard therapy [16]. However, several studies have suggested that abatacept is insufficient in completely alleviating or suppressing T-cell-mediated inflammation in most patients [17, 18]. Moreover, no discernible pattern was observed in the modification of fibrotic lesions in patients with SSc-associated polyarthritis and myopathy who received abatacept treatment [19].

As the role and mechanisms of abatacept in fibrotic diseases remain poorly understood and results are controversial, we conducted a study to investigate its potential anti-fibrosis and anti-inflammatory effects in a HCLO-induced fibrosis model and elucidate the mechanisms of abatacept in this context. In this model, an imbalance between active oxygen and antioxidant systems leads to oxidative stress and the production of free radicals and peroxides, resulting in the development of fibrosis in mice. Our previous research has shown that HCLO-induced fibrosis exhibits systemic vasculopathy, immune cell infiltration, and more extensive fibrosis compared to BLM-induced fibrosis [20]. In this study, we examined the morphological changes, inflammatory cell infiltration and activation of fibroblasts, immune response signature, and altered functional enrichment pathways induced by the administration of abatacept in the HCLO model. Finally, we examined the controlled alterations in immune infiltration in individuals with SSc and HCLO mice who received abatacept treatment.

2 | Methods

2.1 | Animals and Reagents

Six-week-old female BALB/c mice were obtained from Janvier Laboratory (STA, China) and housed in a specific pathogen-free barrier facility, where they received appropriate care in accordance with our institution's guidelines. All chemical agents, except for abatacept (Bristol-Myers Squibb, USA), were acquired from Macklin Agency (Shanghai, China).

2.2 | Experimental Procedure

2.2.1 | HCLO-Induced Fibrosis Mouse Model

The HCLO mice were induced following the protocol outlined in our study [20]. In summary, HCLO was created by mixing NaCLO solution with KH_2PO4 solution (1:110). A total of 200 μL of HCLO and PBS (phosphate-buffered saline) were then subcutaneously administered into specific 1.5 cm^2 areas on the shaven backs of the mice daily for 6 weeks, using a 27-gauge needle ($n = 6$).

2.2.2 | Effects of Abatacept in the HCLO-Induced Mice

To evaluate the ability of abatacept to alleviate fibrotic and inflammatory responses during the mid-stage of HCLO-induced fibrosis, we administered 100 μg of abatacept intraperitoneally to BALB/c mice every other day on day 28 of modeling ($n = 6$). The mice were sacrificed 6 weeks after the first HCLO injection. To ensure adequate drug exposure, we implemented additional abatacept dose groups, including 200 μg/mouse, 400 μg/mouse, and 600 μg/mouse ($n = 4$).

2.3 | Histopathological Analysis

Mouse skin and lung tissues were fixed in a 10% formalin solution for 24–48 h, dehydrated, and embedded in paraffin sections for hematoxylin and eosin (HE) and Masson's trichrome staining. Skin thickness measurement was defined as the mean distance between the epidermis-dermis junction and the dermis-subcutaneous fat junction. Images were captured using an Olympus camera (Shinjuku, Japan), and the skin thickness was assessed by two independent observers.

2.4 | Hydroxyproline Content

The frozen samples including skin and lung tissues were hydrolyzed and analyzed for hydroxyproline content according to the manufacturer's guidelines for the Mak008-1KT kit (Sigma, USA). Each analysis had a calibrated standard curve to determine hydroxyproline content.

2.5 | Immunohistochemical Analysis

Expression levels of CD4, CD8, α-SMA, vimentin, and CD163 were assessed through immunohistochemistry in the skin and lung fragments of the PBS, HCLO, and drug groups. Tissue sections were deparaffinized and underwent antigen retrieval utilizing citric acid repair buffer. Following the inhibition of endogenous peroxidase using 3% H_2O_2 for 25 min, nonspecific binding was blocked for 30 min using 3% bovine serum albumin (BSA). Slides were incubated overnight at 4°C with a mouse monoclonal antibody mixture consisting of anti-CD4, anti-CD8, anti-vimentin, anti-αSMA (Abcam, UK), and anti-CD163 (Servicebio, China), at dilution concentrations of 1:750, 1:1500, 1:750, 1:200, 1:75, and 1:500, respectively. The slides were incubated with an enzyme-labeled goat anti-rabbit

antibody (Servicebio, China) at room temperature for 50 min. Subsequently, they were stained using a diaminobenzidine kit as a chromogenic agent. All slides were examined using a standard bright field microscope from Olympus, located in Shinjuku, Japan. The mean intensity optical density (IOD) was quantified using Image-pro Plus v. 6.0.

2.6 | Analysis of ICOS+ CD3+ T Cells in the Skin, Lung, and Spleen Tissues

Skin from the injection sites underwent digestion in RPMI1640 medium with 2 mg/mL Collagenase IV and 1 mg/mL Disperse II at 37°C for 3–4 h. This was terminated using 4 mL RPMI1640 medium containing 10% FBS, followed by filtration through a 70 μm filter to produce a single-cell suspension of the skin. In addition, lung and spleen tissues were crushed and filtered using a cell strainer. After hypotonic lysis of erythrocytes, we counted cell suspensions from the mentioned three tissues. Subsequently, we incubated the cells with properly labeled antibodies in PBS containing 2% fetal calf serum. To identify CD3+ ICOS+ T cells, we stained them with anti-CD45-BV510, anti-CD3-Percp-Cy5.5, and anti-ICOS-BV421 (BD Biosciences). The cells underwent analysis using a Cytek flow cytometer (BD Biosciences) in accordance with standard protocols. Once analyzed, the resulting data were subjected to analysis using FlowJo software.

2.7 | Analysis of Serum Cytokines

According to the manufacturer's instructions, serum levels of TNF-α, IFN-γ, IL-6, IL-9, IL-10, IL-17A, and IL-22 in mice were determined using the Mouse Inflammation Cytometric Bead Assay (CBA; BD Biosciences, Germany) on a BD FACSCanto II flow cytometer (Cytek).

2.8 | RNA Extraction, Library Construction, and Sequencing Data Analysis

RNA was extracted from skin and lung tissues using TRIzol (Invitrogen Life Technologies, CA, USA) following the manufacturer's protocol. RNA libraries were generated using the NEBNext UltraTM RNA Library Prep Kit from Illumina (NEB, USA) in accordance with the provided instructions. Total RNA and purified library products were measured using the Qubit2.0 Fluorometer and Agilent 2100 bioanalyzer. Paired-end sequences (PE150) were used for the sequencing process on the Illumina HiSeq 3000 platform at Beijing Novogene Co. Ltd. in Beijing, China. Subsequently, the read quality was assessed and clean reads were generated using FastQC software (v0.11.8). Alignment and mapping of sequencing reads were performed using Hisat2 (v2.1.0). The reference genome utilized for mouse datasets was *Mus musculus* GRCm38. The count data were normalized using the "TMM" methodology before calculating DEGs via edgeR (V3.32.0), using the selection criteria of |log-2foldchange| > 1 and a p value of < 0.05. Enriched pathways for DEGs were analyzed using the Gene Set Enrichment Analysis (GSEA) method, with the R package clusterProfiler. The identification of significantly enriched pathways used a threshold of a $p < 0.05$.

2.9 | Deconvolution Analysis to Detect Skin-Infiltrating Cells in SSc Patients and Mice

The analytical tool CIBERSORTx was utilized to determine the fractions of immune cells in mixed cell populations (https://cibersortx.stanford.edu/). This tool allowed for the quantification of immune cell abundance in both SSc patients and the mouse model, using bulk RNA-seq data. The raw RNA-seq data obtained from skin biopsy samples of 47 SSc patients were downloaded from GSE217067. Both the mouse and human datasets were processed in the TPM format. By utilizing the LM22 gene signature matrix for humans and mice [21], we applied B-batch correction, absolute mode, and 1000 permutations to assess the proportions of each cell type.

We then utilized the xCell package to conduct cell type enrichment analysis on 64 immune and stromal cell types, which have been confirmed through in silico simulations and cytometry immunophenotyping [22]. We used xCell to analyze cellular components and markers within tissues from fibrotic models and SSc patients, resulting in diverse cellular expression profiles identified.

2.10 | Statistical Analysis

GraphPad Prism 8 software was utilized to analyze and present the data, excluding bioinformatics data. Unpaired t-tests were performed on numerical variables with normal distributions, while paired T tests were used to evaluate immune cell types and multiple scores in SSc patients between baseline and month 6. For data with non-normal distributions, the Mann–Whitney U test was used. Quantitative data are expressed as mean ± SEM, and statistical significance is considered as $p < 0.05$.

3 | Results

3.1 | Effects of Abatacept on Fibrosis in HCLO-Induced Mice

Compared to the skin tissues from the control group, the HCLO model group showed increased skin thickness, skin swelling, and subcutaneous fat loss. The lung tissue of the model group displayed a disordered structure, and a high volume of inflammatory cells was detected. Furthermore, collagen bundles had formed alongside blood vessels and alveoli. Additionally, the hydroxyproline content of the lungs, which indicates collagen deposition, was considerably higher in the treated HCLO groups compared to the PBS groups.

Based on our previous research [20], we administered 100 μg of abatacept on the first day of week 4 (referred to as "4w") to examine its effects on inflammation and fibrosis, as we had observed a substantial number of inflammatory cells at the 4-week mark in the HCLO-induced skin and lung fibrotic model. Nevertheless, the pathological analysis indicated no substantial amelioration in skin fibrosis within the treatment groups in comparison to the control groups, as evidenced by the deposition of collagen fibers and a reduction in subcutaneous adipose tissue. The drug groups exhibited hyperkeratosis in certain epidermal regions.

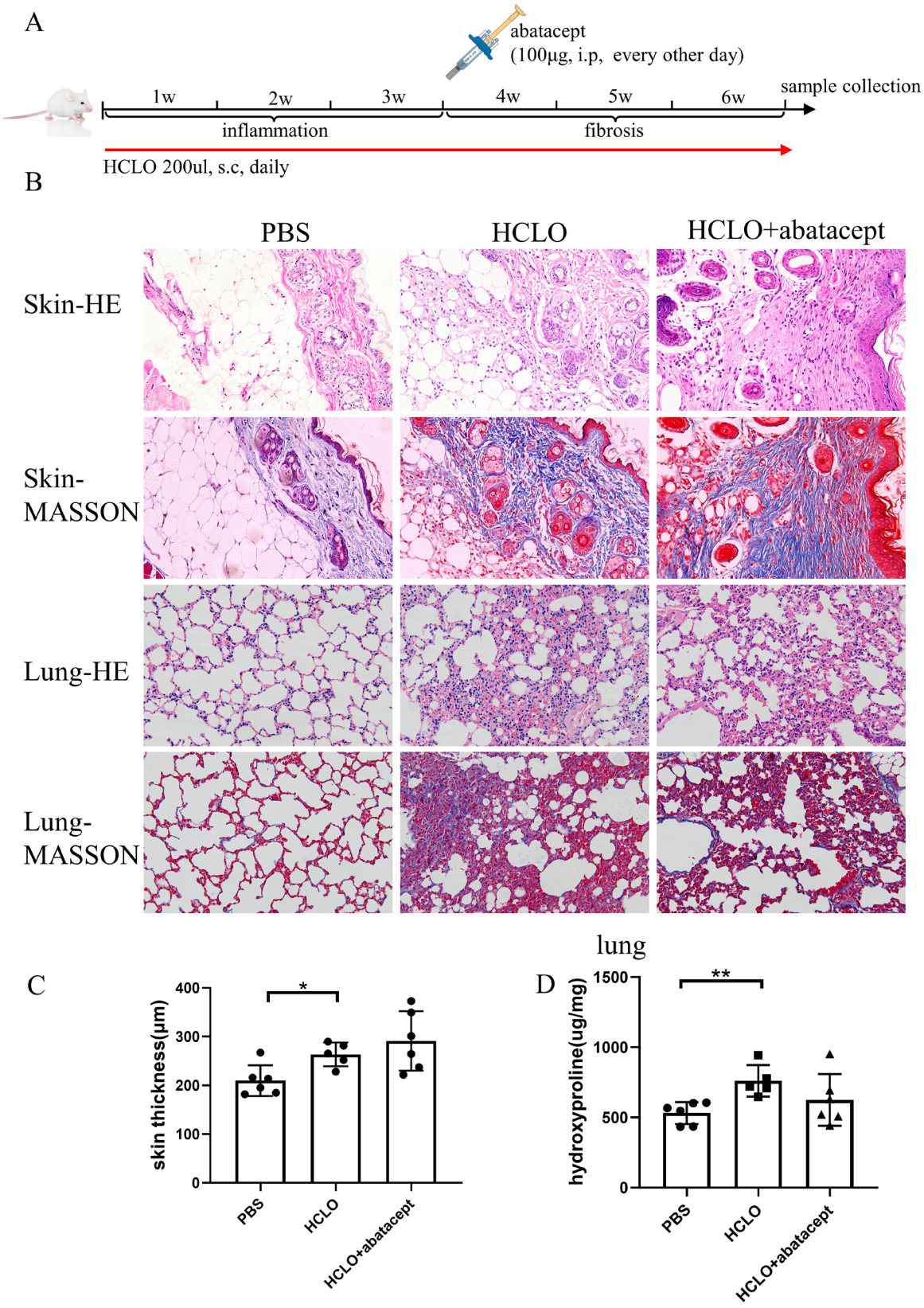

FIGURE 1 | Effects of abatacept on skin and lung fibrosis in hypochlorous acid (HCLO)-induced mice at the time point of the fourth week of modeling. (A) Schematic showing the experimental design and time course of the mouse model. Skin and lung fibrosis was induced by subcutaneous (s.c.) injection of 200ul of HCLO daily for 6 weeks. Abatacept was applied for the last 3 weeks according to the protocol of the animal experiment. (B) Representative skin and lung sections of PBS-injected and HCLO-injected mice from the 6-week experiment, treated with or without abatacept. The scale bar of the panel is 40 μm (magnification, 200X) (C) Assessment of skin thickness after abatacept treatment in the 6-week experiment. (D) Hydroxyproline content after abatacept treatment in the 6-week experiment expressed in μg/mg lung. Values in (C) and (D) are mean ± SEM. $^{*}p \leq 0.05$; $^{**}p \leq 0.01$; $^{***}p \leq 0.001$.

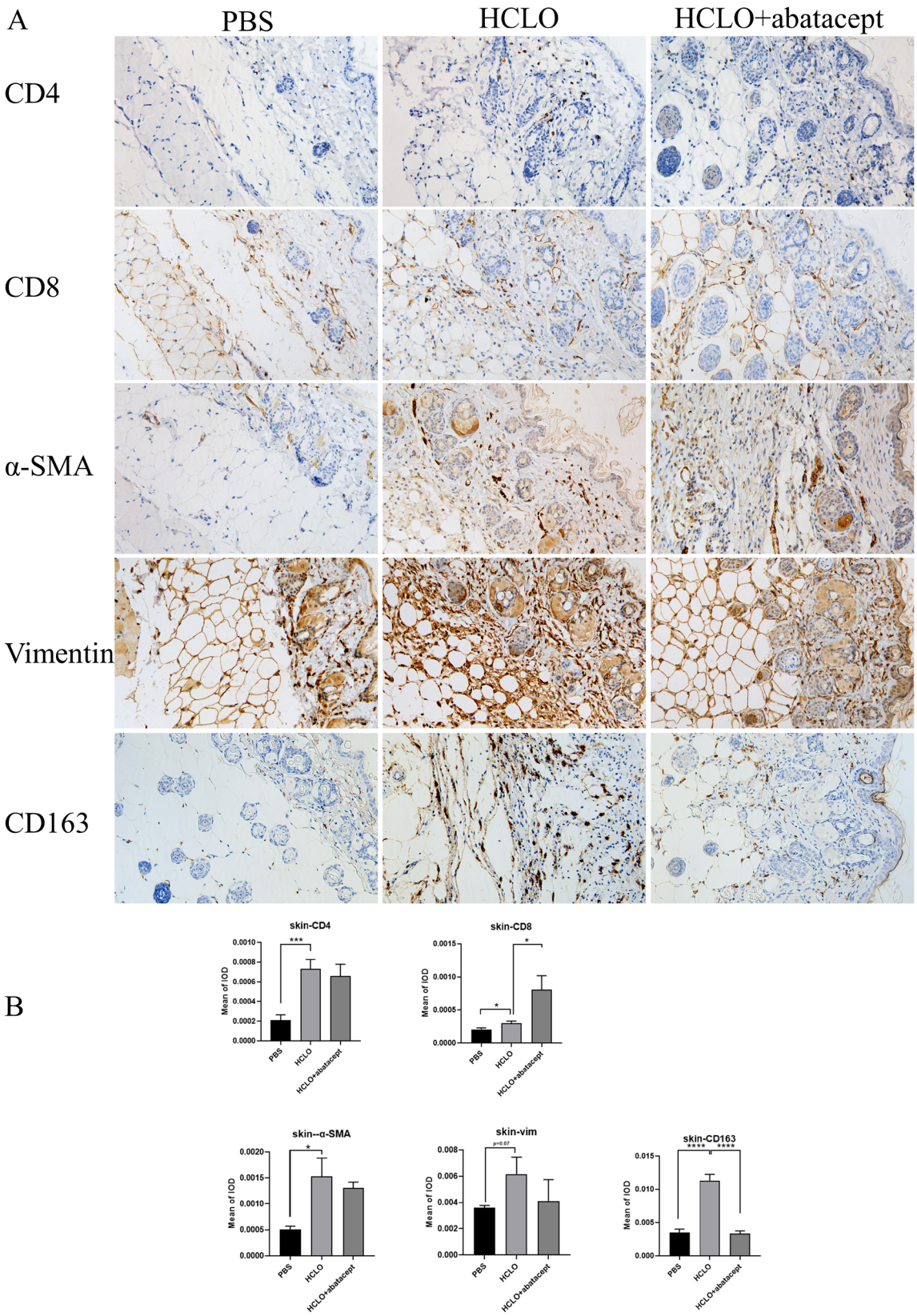

FIGURE 2 | Effects of abatacept on inflammatory cells and myofibroblasts in skin tissue from HCLO mice. (A) Representative IHC staining (brown) of T cells (CD4+/CD8+), myofibroblasts (SMA+/vimentin+), and M2 macrophages (CD163+) on dorsal skin sections counterstained with hematoxylin from PBS, HCLO, and HCLO/abatacept-treated mice. The brown-yellow color means positive staining. The scale bar of the panel is 40 μm (magnification, 200X). (B) Statistical analysis of major immune cells and myofibroblasts in skin tissue (*$p < 0.05$; ***$p < 0.001$; ****$p < 0.0001$. IOD: Integrated optical intensity).

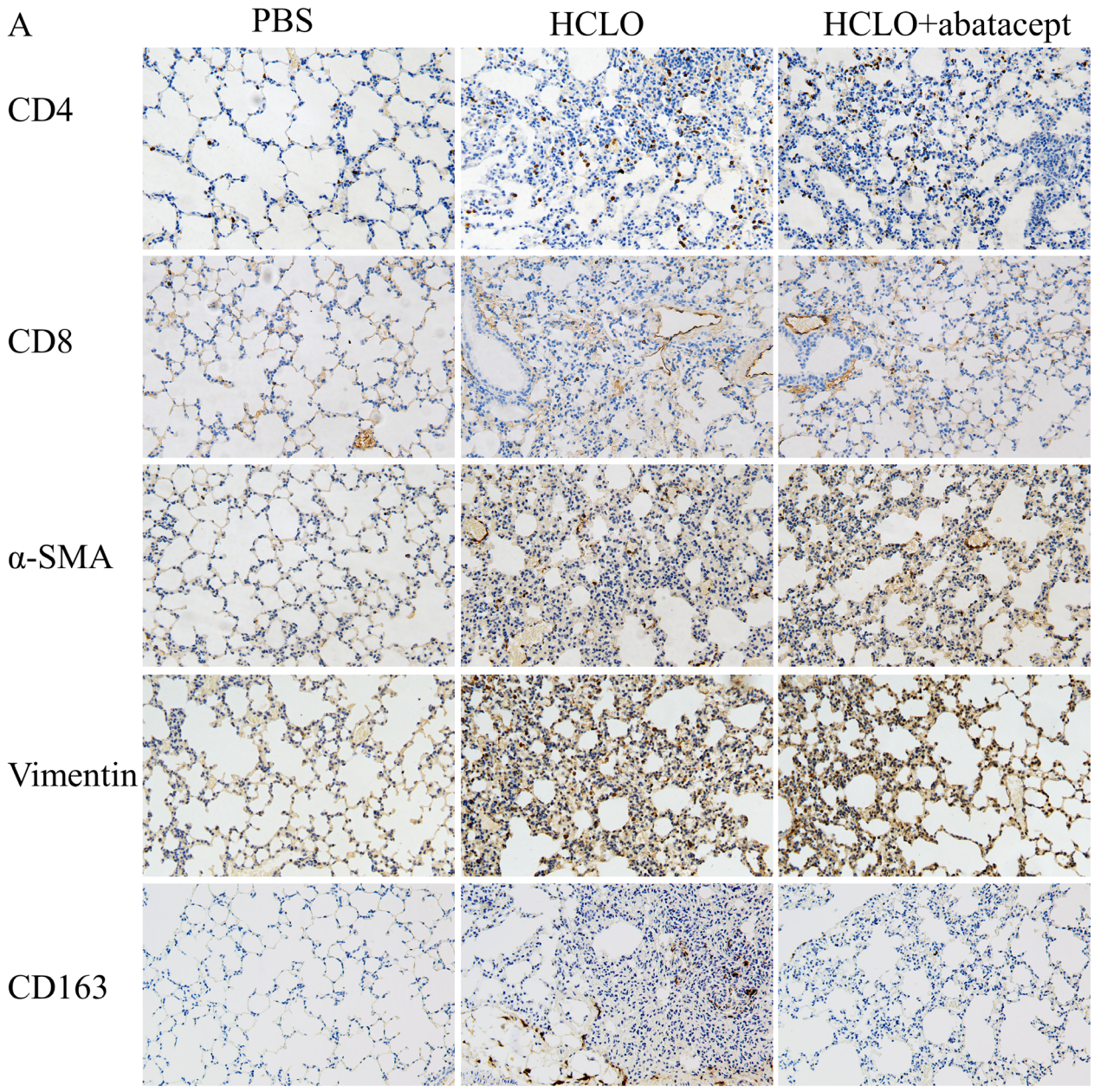

FIGURE 3 | Legend on next page.

FIGURE 3 | Effects of abatacept on inflammatory cells and myofibroblasts in the lung tissue from HCLO mice. (A) Representative IHC staining (brown) of T cells (CD4+/CD8+), myofibroblasts (SMA+/vimentin+), and M2 macrophages (CD163+) on lung tissues counterstained with hematoxylin from PBS, HCLO, and HCLO/abatacept-treated mice. The brown-yellow color means positive staining. The scale bar of the panel is 40 μm (magnification, 200X). (B) Statistical analysis of major immune cells and myofibroblasts in lung tissues (*$p < 0.05$; **$p < 0.01$; ***$p < 0.001$. IOD: Integrated optical intensity).

Moreover, the infiltration of inflammatory cells in the lung tissues of HCLO groups was comparatively higher. However, the drug groups exhibited a slightly lower infiltration rate and decreased tendency. Additionally, there was no significant difference in the hydroxyproline content (Figures 1 and S1).

We additionally set an extra dose of abatacept, including 200 μg/mouse, 400 μg/mouse, and 600 μg/mouse, none of which reduced skin thickness or attenuated pulmonary fibrosis compared with the HCLO group (Figure S2).

3.2 | Effects of Abatacept on the Inflammatory Cells in HCLO-Induced Mice

Previous studies have indicated that an aberrant immune response and fibroblasts have a significant involvement in the development of SSc. In this study, we analyzed the infiltration of inflammatory cells, fibroblasts, and M2 macrophages in the target organs, including the skin and lungs, using immunohistochemistry. The quantities of CD4+ T cells, CD8+ T cells, and CD163+ M2 macrophages within the skin of HCLO models were markedly elevated compared to the control group, specifically within the dermal layer and subcutaneous tissue layer, although the variance from the abatacept group was insignificant excluding M2 macrophages. Also, the manifestation of α-SMA and vimentin, which indicate the number of myofibroblasts, had amplified within the model in comparison to control mice. However, no difference was observed between the model and drug groups (Figures 2 and S3). In the lung tissue, there was a significant infiltration of inflammatory cells (CD4+ T cells, CD8+ T cells, and M2 macrophages) as well as myofibroblasts in the model group. The results in the lung tissue of the medical group were comparable to those in the skin (Figure 3 and S4). The results indicated that abatacept has some degree of anti-inflammatory activity and has had no effect on fibroblast activation in either skin or lung tissue.

We further measured the levels of cytokines important in the fibrosis process in the HCLO mouse model after abatacept administration. Compared with control mice, HCLO mice exhibited significantly increased levels of TNF-α, IFN-γ, IL-6, IL-9, IL-10, and IL-22; mice treated with abatacept showed significantly decreased levels of IL-6. No differences in the levels of TNF-α, IFN-γ, IL-9, IL-10, and IL-22 were observed (Figure S5).

3.3 | Effects of Abatacept on the CD28-Dependent Signaling and Immune Response Signature in HCLO-Induced Mice

In addition to assessing the anti-fibrogenic and anti-inflammatory activities of abatacept in vivo, we also performed RNA-seq analysis of skin and lung tissues to investigate the potential and broader effects of abatacept on HCLO-modulated gene expression. The volcano plot illustrated the differentially expressed genes (DEGs) in both skin and lung tissues between the drug and model groups (Figure 4A,C). As the function of abatacept is to inhibit the activation of CD28-dependent T lymphocytes, we primarily observed a reduction in gene expression associated with T lymphocyte activation, specifically CD28-dependent signaling. The results of the heatmap analysis revealed a significant improvement in the expression of various genes involved in immune activation, such as *Cd84*, *Cd80*, *Ctla4*, *Cd86*, *Icos*, and *Cd28*, within the drug group when compared to that of the lung and skin tissues of the HCLO group. They also included chemokine ligands and receptors (*Ccl7*), adhesion molecules (*BCAM*), complement components (*C3*), and other genes engaged in the immune system (Figure 4A–D). ICOS is a T-cell costimulatory molecule and part of the CD28 co-stimulatory signal, and CD28 dose-dependently induces ICOS [23]. The ICOS expression analysis via flow cytometry supported the findings of RNA-seq analysis. Following abatacept treatment, the proportion of ICOS in CD3+ T cells was significantly reduced in three tissues, including skin, lung, and spleen, compared to HCLO mice (Figure 4E,F).

3.4 | The Potential Mechanisms of Abatacept in HCLO-Induced Mice

We complemented the GSEA analysis with the full set of genes in the skin and lung tissues of all groups. The administration of HCLO led to substantial alterations in several pathways in the skin lesions, including remodeling of fibrotic tissue, inflammation, profibrotic signaling, angiogenesis, metabolism, and cell death. It is noteworthy that abatacept further aggravated the processes of epidermis and skin development, similar to the results of the HE. On the other hand, several immune response pathways were reduced in the drug group compared to the model group, including myeloid leukocyte-mediated immunity, B-cell activation and proliferation, and lymphocyte chemotaxis. Regrettably, abatacept failed to impact lipid balance, vasculogenesis, metabolism, and cell death affected by HCLO, except for a noted increase in vascular permeability (Figure 5A). The GSEA findings revealed that the genes in the lung tissue of the HCLO group were primarily associated with fibrotic tissue remodeling, inflammation, profibrotic signaling, angiogenesis, metabolism, cell death, and response to low oxygen levels. Furthermore, the abatacept group exhibited a decrease in several signaling pathways such as ECM organization, epithelial migration, regulation of macrophage activation, mucosal innate immune response, lipid localization, and response to hypoxia. Furthermore, the drug had a partial impact on angiogenesis and did not affect fibrosis pathways and cell death (Figure 5B). RNA-seq analysis indicated that mice treated with abatacept exhibited a reduced

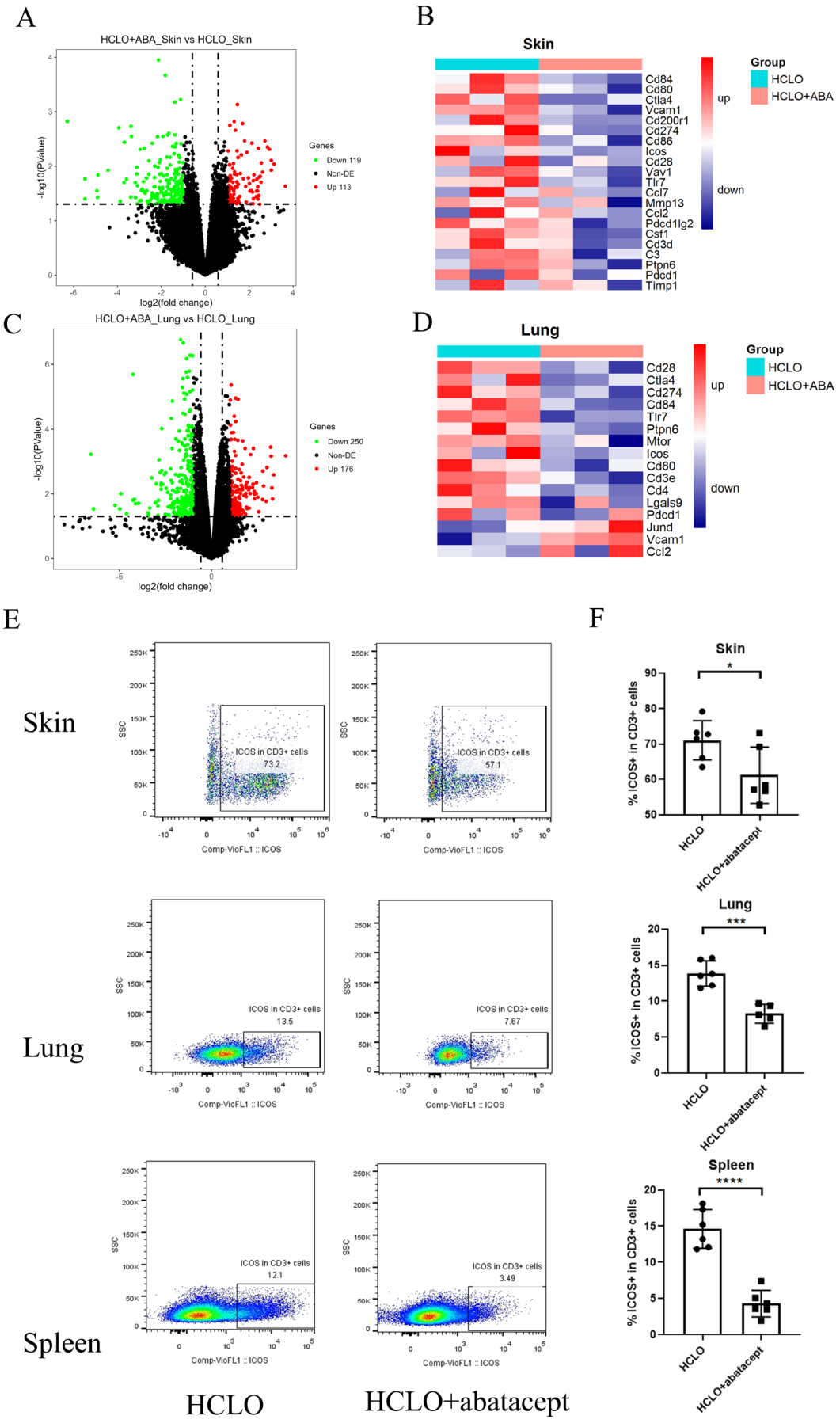

FIGURE 4 | Legend on next page.

FIGURE 4 | Effects of abatacept on the CD28-dependent signaling and immune response signature in the HCLO model. (A and C) Volcano plot showing differentially expressed genes in skin and lung tissues by RNA-seq. Genes up or downregulated by > 2-fold and $p < 0.05$ are shown in red and green, respectively. (B and D) Hierarchical clustering of core enrichment genes in skin and lung tissues of the HCLO model and the abatacept (ABA) group from the costimulation of the CD28 family and the immune response signature. (E) Representative flow plots of ICOS in CD3+ T cells in skin, lung, and spleen of HCLO model and abatacept group. (F) The summarized percentages of ICOS in CD3+ T cells in skin, lung, and spleen of HCLO model and abatacept group. Values in (F) are mean ± SEM. *$p \leq 0.05$; **$p \leq 0.01$; ***$p \leq 0.001$; ****$p < 0.0001$.

immune activation signature in skin and lung tissues, and less ECM organization and angiogenesis in lung tissues after HCLO induction.

3.5 | Effects of Abatacept on Immune Infiltration in SSc Patients and HCLO-Induced Mice

To more fully evaluate the proportions of immune cells after administering abatacept, we first used CIBERSORTx to deconvolute our RNA-seq data of skin and lung tissues. Notably, abatacept significantly reduced M2 macrophages in skin tissues compared to HCLO mice, while the remaining immune cells showed no significant changes. In lung tissues, both M2 macrophages and monocytes demonstrated a considerable reduction in the abatacept-treated HCLO group when compared to the model groups (Figure 6A). Furthermore, a comparable analysis was conducted on an SSc group treated with abatacept (comprising of 47 SSc patients at both baseline and after 6 months of treatment). A comprehensive study was performed based on the grouping system outlined in the article [24], examining the alterations in immune cells within intrinsic molecular subsets of SSc patients, including the inflammatory subsets, the fibroproliferative subsets, the normal-like subsets, and the limited subsets. The study revealed that the subset of patients with inflammatory improvers had a significant decrease in the ratio of M2 macrophages and monocytes between the baseline and 6-month time points. Furthermore, the proportion of patients with nonimproving inflammation showed a declining trend of M2 macrophages. These results align with our histochemical findings. It is worth noting that these cells were not significantly present in the normal-like and fibroproliferative subsets of patients (Figure 6A).

We conducted a thorough analysis of various scores after administering abatacept treatment to both the fibrosis model and SSc patients using xCell analysis. We observed a decrease in immune and microenvironmental scores in both skin and lung tissue from the HCLO model and in the inflammatory subset of SSc patients after drug treatment (Figure 6B).

4 | Discussion

Although the exact pathogenesis is not fully understood, a better understanding of the pathogenic mechanism underlying SSc and appropriate therapeutic agents is essential [25, 26]. Consistent with our previously published study, we found that the proportions of CD4+ T cells, CD8+ T cells, and myofibroblasts were increased in the skin and lung tissues of HCLO-induced mice [20]. In this study, abatacept did not reduce the ratio of lymphocytes and myofibroblasts. In addition, abatacept treatment failed to reduce skin and lung fibrosis induced by subcutaneous injection of HCLO. Notably, we observed a reduction in CD28 costimulation and the immune response signature in HCLO-induced mice treated with abatacept. Abatacept also reduced the proportion of M2 macrophages in both skin and lung tissues.

Dysregulation of innate and adaptive immunity plays a significant role in SSc. Abnormal inflammatory cells and features exist in target tissues such as skin and lungs, while the number and functions of immune cells are altered [27]. Previous studies have indicated a decline in the CD28 gene family among clinical improvers receiving abatacept between baseline and 6 months [24]. ICOS is expressed on activated T cells and is also significantly reduced as a key enrichment gene for CD28 family costimulation. However, there were no significant changes in abatacept-treated nonresponders. When the patient population with SSc was stratified according to intrinsic subsets, the trend was further clarified in the inflammatory subset that improved with abatacept, rather than in the fibroproliferative or normal-like subsets [24]. In a separate investigation, the proportion of ICOS-positive T cells in relation to total CD3-positive T cells was significantly diminished in the skin lesions of the abatacept-treated model group when contrasted with control IgG1 mice [28]. Our findings corroborate this impact of T-cell deactivation, whereby a decrease in CD28 signaling and the ratio of ICOS+ CD3+ T cells in skin, lung, and spleen tissues was witnessed after abatacept administration. This outcome could potentially be linked to the mechanism of action of abatacept, which facilitates costimulatory blockade, thus restraining hyperactivated T-cell subsets.

The innate immune response has been observed to be activated at various stages of SSc [29, 30]. In fact, activated M2 macrophages that are present in the blood and target organs exhibit an essential pathogenetic role, demonstrating both anti-inflammatory and pro-fibrotic attributes [31]. A prior examination revealed that there was a significant reduction in the number of monocytes (CD68+) in the lesional skin of BLM-induced mice treated with abatacept compared to those injected with control IgG1 [28]. In the lungs affected by lesions in the Fra-2 transgenic mouse model, which demonstrates systemic fibrosis, microangiopathy, and pulmonary hypertension, the administration of abatacept was found to significantly decrease the proportion of M2 macrophages (cMAF, arginase, and F4/80) to overall macrophages [32]. Additionally, acazicolcept, a dual ICOS/CD28 antagonist, lowered the number of macrophages (CD68+) infiltrating the fibrotic skin of the HCLO model [33]. The immune infiltration pattern was assessed with CIBERSORTx, revealing that the percentage of M2 macrophages in the skin biopsy of the inflammatory subset that responded to abatacept was substantially reduced at 6 months compared to baseline (GSE217067) [24]. Similarly, there was a noteworthy decrease in the percentage of M2 cells in the skin and lungs of the abatacept-treated model

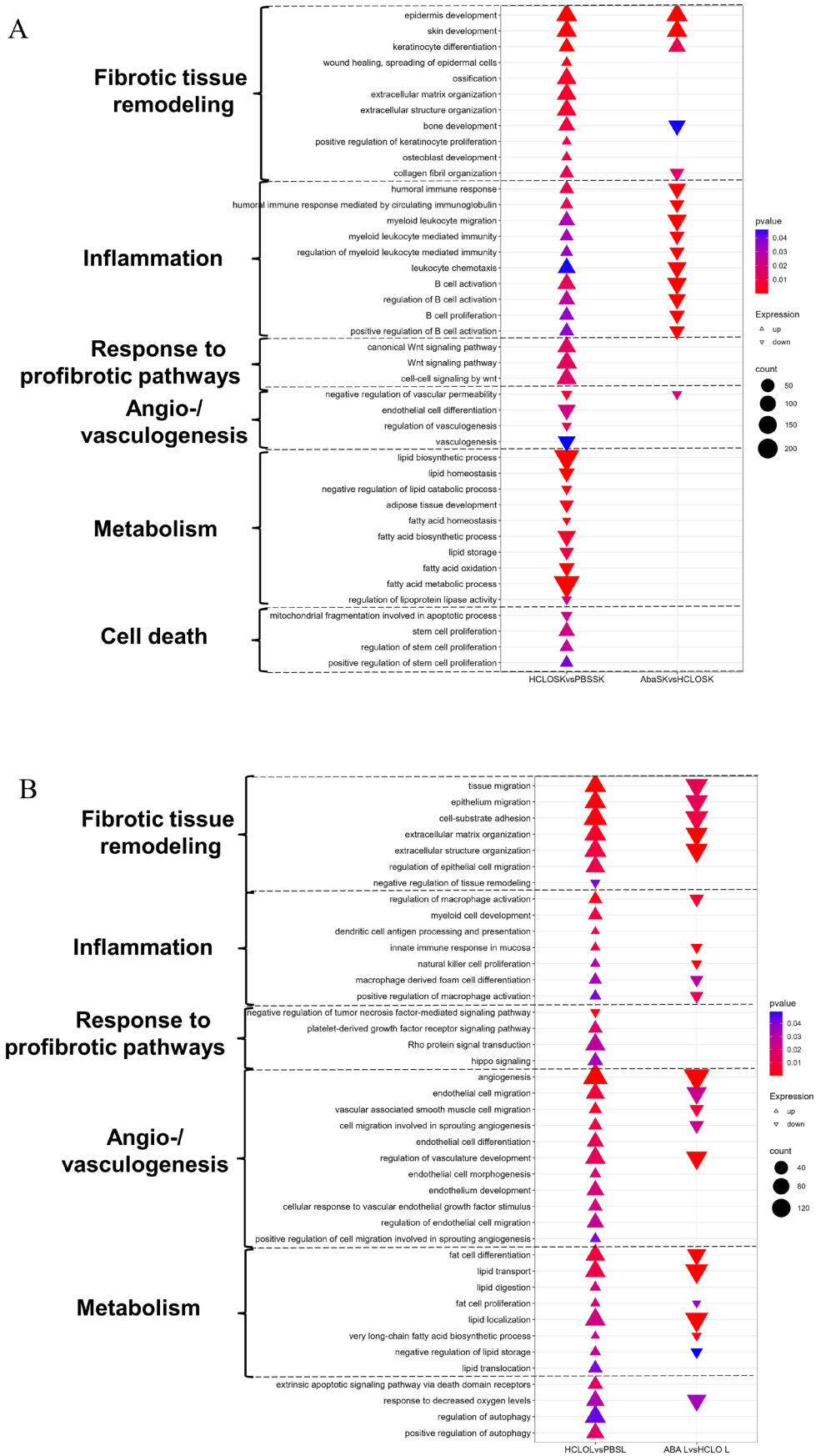

FIGURE 5 | Functional analysis of abatacept on pathways regulated by the HCLO model. Significant pathways show the effects of abatacept on skin (A) and lung (B) tissues of the HCLO model by GSEA functional enrichment analysis. The color depth represents the *p* value. The area of the circles in the graph indicates the number of genes.

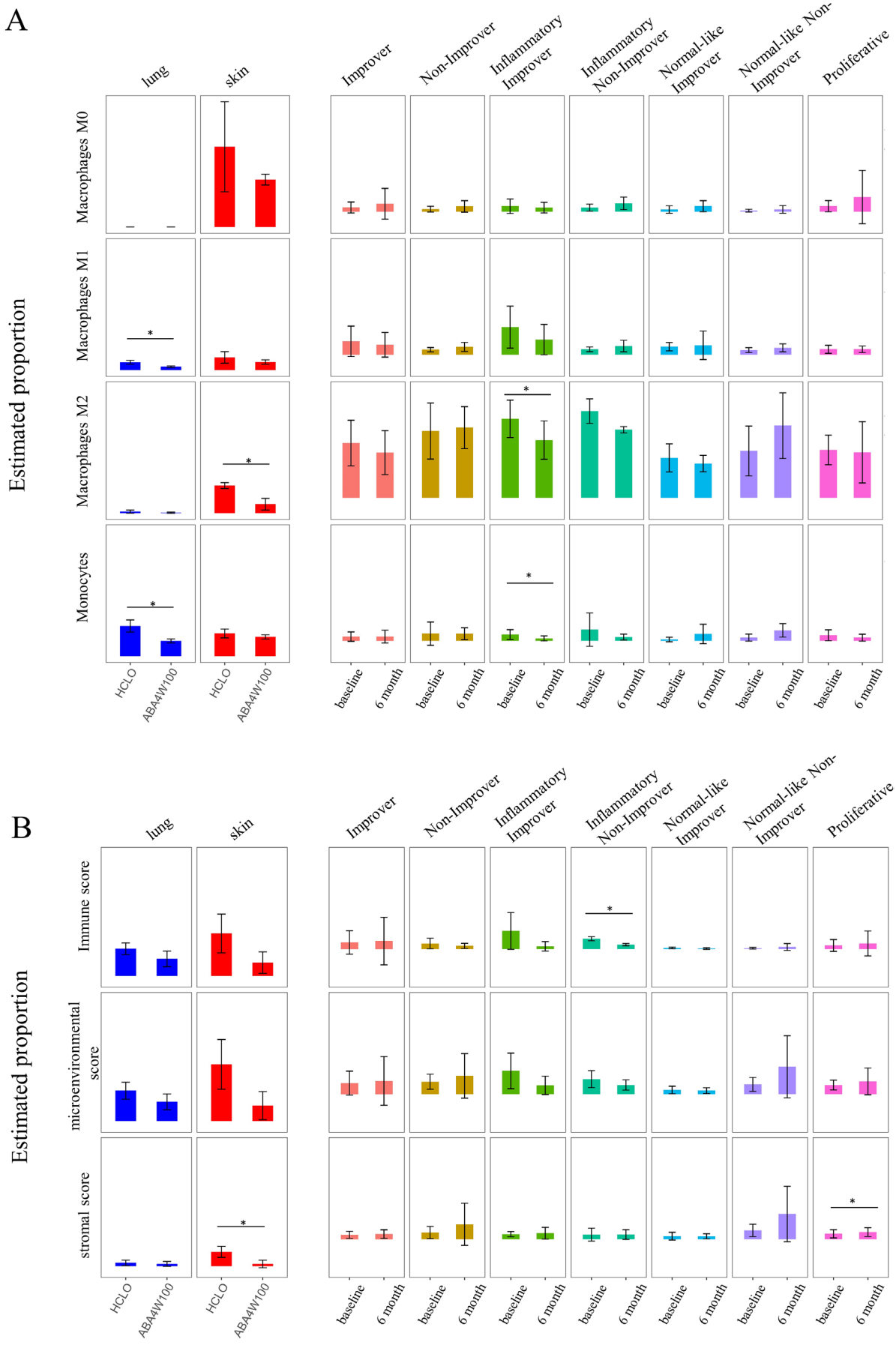

FIGURE 6 | Legend on next page.

FIGURE 6 | Effects of abatacept on immune infiltration in HCLO mice and systemic sclerosis (SSc) patients (GSE217067). (A) Histograms showing the representative infiltrating immune cells in the skin and lung tissues of HCLO and in the skin of medical SSc patients at both baseline and after 6 months of treatment, including abatacept improver, abatacept nonimprover, inflammatory abatacept improver, inflammatory abatacept nonimprover, normal-like abatacept improver, normal-like abatacept nonimprover, and proliferative abatacept improver by CIBERSORTx analysis. (B) Histograms showing the proportion of multiple scores in the skin and lung tissues of HCLO and in the skin of medical SSc patients at both baseline and after 6 months of treatment, including abatacept improver, abatacept nonimprover, inflammatory abatacept improver, inflammatory abatacept nonimprover, normal-like abatacept improver, normal-like abatacept nonimprover, and proliferative abatacept improver by xCell analysis. *$p < 0.05$.

group. This result paralleled the discovery of considerably diminished $CD163^{+}M2$ macrophages in the skin and lung tissue of the treated mice compared to the model group, as demonstrated by immunohistochemistry. These findings support the view that abatacept treatment attenuates inflammatory pathways.

However, dermal thickening and collagen deposition in the target area of the HCLO model were not reduced by abatacept in our study, nor was the number of myofibroblasts. A 2022 Phase II randomized controlled trial (NCT02161406) involving 88 SSc patients yielded noteworthy findings. While no significant difference in MRSS was observed between the abatacept and control groups overall, subgroup analysis based on gene expression phenotypes revealed that only the inflammatory subgroup showed a significant reduction in MRSS after abatacept treatment. By contrast, the fibroproliferative subgroups exhibited no differences. These findings underscore the heterogeneity of SSc, and abatacept may only exert its therapeutic effect when cases are stratified based on intrinsic gene expression subsets and targeted accordingly [34]. After 11 months of treatment with abatacept in another clinical trial, SSc patients with refractory polyarthritis showed significant improvement in joint parameters and met EULAR good response criteria. However, there was no significant improvement in muscle outcome indicators in SSc myopathy, and there was no observed trend in skin or lung fibrosis after being treated with abatacept [19]. These studies suggested that inhibiting the CD28 pathway alone may not have a significant impact on fibrotic skin lesions in SSc patients. In fact, activated T cells often downregulate CD28 and become less dependent on CD28 co-stimulation, and CD28-negative T cells accumulate in various autoimmune diseases. The quantity of specific CD28-negative T cells correlates with disease activity and damage indexes, which are also predictive of clinical response to abatacept in patients with rheumatoid arthritis [35–38].

Abatacept has been administered in preclinical mouse models. The drug prevented and induced regression of inflammation-induced skin fibrosis in BLM-injected mice, and the control in this study was human IgG1 [28]. Nevertheless, a separate study on the effect of abatacept in mice with heart failure found evidence indicating that the administration of human Ig could be immunogenic in mice. The use of IgG control may exacerbate the inflammatory response induced by transverse aortic constriction and also create the appearance of a greater protective effect in the abatacept group, which is why PBS was used as a control in this study [39]. Furthermore, it was found that abatacept had no impact on fibrosis in either CB17-SCID or TSK-1 mice. The former does not possess T cells, while the latter operates as an inflammation-independent mouse model. Consequently, the anti-fibrosis effect of abatacept may require T cells [28]. Previous research indicates that elevated indicators of oxidative stress and reduced levels of antioxidant components are present in individuals with SSc [40]. These factors have been linked to the disease progression and modified Rodnan skin score (mRSS), renal vascular injury, and level of lung fibrosis [41–45]. Furthermore, certain therapeutic agents have been found to selectively reduce specific ROS components or have no impact at all [43]. The potential pathogenesis of HCLO in the skin and lungs of mice differs and is independent of the immune system. First, the copious ROS provided by HCLO acts directly on fibroblasts, activating the Ras pathway, which induces collagen synthesis in skin tissue. Recent research has demonstrated that ROS acts on numerous targets in SSc. Activation of endothelial cells leads to increased vascular reactivity, impaired angiogenesis, differentiation and proliferation of fibroblasts, and organization of the ECM. Conversely, ROS also promotes autoimmunity and chronic inflammation through the creation of neoepitopes and activation of lymphocytes and macrophages. The tissue damage directly caused by oxidative stress may bypass the involvement of T cells. An active loop exists in SSc that sustains ROS production and transduction. The mechanism and timing of abatacept during mid-phase induction may explain the unrelieved skin fibrosis directly caused by oxidative stress. In light of these results, it is suggested that rather than fibrosis, the costimulation blocker abatacept may be more advantageous in correcting the immune response induced by HCLO.

To the best of our knowledge, our study was the first in vivo experiment of abatacept in a preclinical model of murine HCLO-induced fibrosis, and RNA-seq analysis allowed us to comprehensively analyze the mechanism of abatacept in HCLO-induced skin and lung fibrosis. The findings have verified the inhibitory impact of abatacept on the CD28 pathway and immune response established in earlier investigations [24], which endorses the potential application of this drug in the treatment of other diseases with abnormal immune response. At the same time, this study confirmed the previous findings on HCLO modeling mechanism [46] and encouraged researchers to select appropriate animal models with specific modeling mechanisms for different drugs.

This study has limitations. Our study only concentrates on HCLO-induced fibrosis mice to investigate the efficacy and mechanism of abatacept. There are several fibrosis models currently available that mimic SSc, each exhibiting distinct characteristics. Additional studies may be conducted in other models to better understand the effects and mechanisms of abatacept in SSc in the future.

In conclusion, abatacept demonstrated an immunosuppressive effect on the skin and lungs of HCLO models, as evidenced by a reduction in CD28 signaling and a decrease in the proportion of M2 macrophages. However, abatacept did not decrease collagen

deposition and fibroblast activation in the skin and lungs of HCLO-induced mice.

Author Contributions

Bingying Dai: writing – review and editing, writing – original draft, visualization, validation, methodology, investigation, formal analysis. **Meng Meng:** methodology, investigation, validation. **Weilin Chen:** methodology, investigation. **Junyu Zhou:** methodology. **Qiming Meng:** methodology. **Liqing Ding:** investigation. **Shasha Xie:** software, visualization. **Ding Bao:** investigation. **Xiaojing Li:** methodology. **Lijuan Zhao:** investigation. **Ting Huang:** methodology. **Chunliu Lv:** resources. **Hui Luo:** resources, funding acquisition. **Sijia Liu:** supervision, formal analysis, funding acquisition. **Honglin Zhu:** supervision, writing – review and editing, project administration, conceptualization.

Ethics Statement

This study was carried out according to the recommendations of the Ethics Committee of Xiangya Hospital of Central South University. The protocol was approved by the Ethics Committee of Xiangya Hospital of Central South University.

Conflicts of Interest

The authors declare no conflicts of interest.

Data Availability Statement

The data that support the findings of this study are available from the corresponding author upon reasonable request.

References

1. Y. Asano, "Systemic Sclerosis," *Journal of Dermatology* 45, no. 2 (2018): 128–138.

2. C. P. Denton and D. Khanna, "Systemic Sclerosis," *Lancet* 390, no. 10103 (2017): 1685–1699.

3. H. Zhu, H. Luo, B. Skaug, et al., "Fibroblast Subpopulations in Systemic Sclerosis: Functional Implications of Individual Subpopulations and Correlations With Clinical Features," *Journal of Investigative Dermatology* 144, no. 6 (2024): 1251–1261.

4. W. Jin, Y. Zheng, and P. Zhu, "T Cell Abnormalities in Systemic Sclerosis," *Autoimmunity Reviews* 21, no. 11 (2022): 103185.

5. N. Higashi-Kuwata, M. Jinnin, T. Makino, et al., "Characterization of Monocyte/Macrophage Subsets in the Skin and Peripheral Blood Derived From Patients With Systemic Sclerosis," *Arthritis Research & Therapy* 12, no. 4 (2010): R128.

6. B. Dai, L. Ding, L. Zhao, H. Zhu, and H. Luo, "Contributions of Immune Cells and Stromal Cells to the Pathogenesis of Systemic Sclerosis: Recent Insights," *Frontiers in Pharmacology* 13 (2022): 826839.

7. D. Xue, T. Tabib, C. Morse, et al., "Expansion of Fcgamma Receptor IIIa-Positive Macrophages, Ficolin 1-Positive Monocyte-Derived Dendritic Cells, and Plasmacytoid Dendritic Cells Associated With Severe Skin Disease in Systemic Sclerosis," *Arthritis & Rheumatism* 74, no. 2 (2022): 329–341.

8. S. Bhattacharyya, J. Wei, and J. Varga, "Understanding Fibrosis in Systemic Sclerosis: Shifting Paradigms, Emerging Opportunities," *Nature Reviews Rheumatology* 8, no. 1 (2011): 42–54.

9. J. E. Mouawad and C. Feghali-Bostwick, "The Molecular Mechanisms of Systemic Sclerosis-Associated Lung Fibrosis," *International Journal of Molecular Sciences* 24, no. 3 (2023): 2963.

10. J. H. Esensten, Y. A. Helou, G. Chopra, A. Weiss, and J. A. Bluestone, "CD28 Costimulation: From Mechanism to Therapy," *Immunity* 44, no. 5 (2016): 973–988.

11. B. M. Carreno, F. Bennett, T. A. Chau, et al., "CTLA-4 (CD152) can Inhibit T Cell Activation by Two Different Mechanisms Depending on Its Level of Cell Surface Expression," *Journal of Immunology* 165, no. 3 (2000): 1352–1356.

12. L. Moreland, G. Bate, and P. Kirkpatrick, "Abatacept," *Nature Reviews. Drug Discovery* 5, no. 3 (2006): 185–186.

13. J. Romo-Tena, D. Gomez-Martin, and J. Alcocer-Varela, "CTLA-4 and Autoimmunity: New Insights Into the Dual Regulator of Tolerance," *Autoimmunity Reviews* 12, no. 12 (2013): 1171–1176.

14. J. S. Smolen, R. B. M. Landewé, S. A. Bergstra, et al., "EULAR Recommendations for the Management of Rheumatoid Arthritis With Synthetic and Biological Disease-Modifying Antirheumatic Drugs: 2022 Update," *Annals of the Rheumatic Diseases* 82, no. 1 (2023): 3–18.

15. X. Zhou, H. Cao, S. Y. Fang, et al., "CTLA-4 Tail Fusion Enhances CAR-T Antitumor Immunity," *Nature Immunology* 24, no. 9 (2023): 1499–1510.

16. S. C. Li, K. S. Torok, S. S. Ishaq, et al., "Preliminary Evidence on Abatacept Safety and Efficacy in Refractory Juvenile Localized Scleroderma," *Rheumatology (Oxford)* 60, no. 8 (2021): 3817–3825.

17. P. Masson, L. Henderson, J. R. Chapman, J. C. Craig, A. C. Webster, and Cochrane Kidney and Transplant Group, "Belatacept for Kidney Transplant Recipients," *Cochrane Database of Systematic Reviews* 2014, no. 11 (2014): CD010699.

18. J. A. Singh, A. Hossain, E. Tanjong Ghogomu, et al., "Biologics or Tofacitinib for People With Rheumatoid Arthritis Unsuccessfully Treated With Biologics: A Systematic Review and Network Meta-Analysis," *Cochrane Database of Systematic Reviews* 3, no. 3 (2017): CD012591, https://doi.org/10.1002/14651858.CD012591.

19. M. Elhai, M. Meunier, M. Matucci-Cerinic, et al., "Outcomes of Patients With Systemic Sclerosis-Associated Polyarthritis and Myopathy Treated With Tocilizumab or Abatacept: A EUSTAR Observational Study," *Annals of the Rheumatic Diseases* 72, no. 7 (2013): 1217–1220.

20. M. Meng, J. Tan, W. Chen, et al., "The Fibrosis and Immunological Features of Hypochlorous Acid Induced Mouse Model of Systemic Sclerosis," *Frontiers in Immunology* 10 (2019): 1861.

21. Z. Chen, A. Huang, J. Sun, T. Jiang, F. X. F. Qin, and A. Wu, "Inference of Immune Cell Composition on the Expression Profiles of Mouse Tissue," *Scientific Reports* 7 (2017): 40508.

22. D. Aran, Z. Hu, and A. J. Butte, "xCell: Digitally Portraying the Tissue Cellular Heterogeneity Landscape," *Genome Biology* 18, no. 1 (2017): 220.

23. C. J. Wang, F. Heuts, V. Ovcinnikovs, et al., "CTLA-4 Controls Follicular Helper T-Cell Differentiation by Regulating the Strength of CD28 Engagement," *Proceedings of the National Academy of Sciences of the United States of America* 112, no. 2 (2015): 524–529.

24. B. K. Mehta, M. E. Espinoza, J. M. Franks, et al., "Machine-Learning Classification Identifies Patients With Early Systemic Sclerosis as Abatacept Responders via CD28 Pathway Modulation," *JCI Insight* 7, no. 24 (2022): 155282, https://doi.org/10.1172/jci.insight.155282.

25. D. A. Gyftaki-Venieri, D. J. Abraham, and M. Ponticos, "Insights Into Myofibroblasts and Their Activation in Scleroderma: Opportunities for Therapy?," *Current Opinion in Rheumatology* 30, no. 6 (2018): 581–587.

26. H. Bukiri and E. R. Volkmann, "Current Advances in the Treatment of Systemic Sclerosis," *Current Opinion in Pharmacology* 64 (2022): 102211.

27. D. Fang, B. Chen, A. Lescoat, D. Khanna, and R. Mu, "Immune Cell Dysregulation as a Mediator of Fibrosis in Systemic Sclerosis," *Nature Reviews Rheumatology* 18, no. 12 (2022): 683–693.

28. M. Ponsoye, C. Frantz, N. Ruzehaji, et al., "Treatment With Abatacept Prevents Experimental Dermal Fibrosis and Induces Regression of Established Inflammation-Driven Fibrosis," *Annals of the Rheumatic Diseases* 75, no. 12 (2016): 2142–2149.

29. A. Hejrati, A. Rafiei, M. Soltanshahi, et al., "Innate Immune Response in Systemic Autoimmune Diseases: A Potential Target of Therapy," *Inflammopharmacology* 28, no. 6 (2020): 1421–1438.

30. N. H. Servaas, J. Spierings, A. Pandit, and J. M. van Laar, "The Role of Innate Immune Cells in Systemic Sclerosis in the Context of Autologous Hematopoietic Stem Cell Transplantation," *Clinical and Experimental Immunology* 201, no. 1 (2020): 34–39.

31. V. K. Raker, Y. O. Kim, J. Haub, et al., "Myeloid Cell Populations and Fibrogenic Parameters in Bleomycin- and HOCl-Induced Fibrosis," *Experimental Dermatology* 25, no. 11 (2016): 887–894, https://doi.org/10.1111/exd.13124.

32. G. Boleto, C. Guignabert, S. Pezet, et al., "T-Cell Costimulation Blockade Is Effective in Experimental Digestive and Lung Tissue Fibrosis," *Arthritis Research & Therapy* 20, no. 1 (2018): 197.

33. C. Orvain, A. Cauvet, A. Prudent, et al., "Acazicolcept (ALPN-101), a Dual ICOS/CD28 Antagonist, Demonstrates Efficacy in Systemic Sclerosis Preclinical Mouse Models," *Arthritis Research & Therapy* 24, no. 1 (2022): 13.

34. D. Khanna, C. Spino, S. Johnson, et al., "Abatacept in Early Diffuse Cutaneous Systemic Sclerosis: Results of a Phase II Investigator-Initiated, Multicenter, Double-Blind, Randomized, Placebo-Controlled Trial," *Arthritis & Rheumatism* 72, no. 1 (2020): 125–136, https://doi.org/10.1002/art.41055.

35. M. Scarsi, T. Ziglioli, and P. Airo, "Baseline Numbers of Circulating CD28-Negative T Cells May Predict Clinical Response to Abatacept in Patients With Rheumatoid Arthritis," *Journal of Rheumatology* 38, no. 10 (2011): 2105–2111.

36. S. Piantoni, F. Regola, A. Zanola, et al., "Effector T-Cells Are Expanded in Systemic Lupus Erythematosus Patients With High Disease Activity and Damage Indexes," *Lupus* 27, no. 1 (2018): 143–149.

37. D. Schmidt, J. J. Goronzy, and C. M. Weyand, "CD4+ CD7- CD28- T Cells Are Expanded in Rheumatoid Arthritis and Are Characterized by Autoreactivity," *Journal of Clinical Investigation* 97, no. 9 (1996): 2027–2037.

38. D. Mou, J. Espinosa, D. J. Lo, and A. D. Kirk, "CD28 Negative T Cells: Is Their Loss Our Gain?," *American Journal of Transplantation* 14, no. 11 (2014): 2460–2466.

39. M. Kallikourdis, E. Martini, P. Carullo, et al., "T Cell Costimulation Blockade Blunts Pressure Overload-Induced Heart Failure," *Nature Communications* 8 (2017): 14680.

40. J. Y. Luo, X. Liu, M. Jiang, H. P. Zhao, and J. J. Zhao, "Oxidative Stress Markers in Blood in Systemic Sclerosis: A Meta-Analysis," *Modern Rheumatology* 27, no. 2 (2017): 306–314.

41. A. Servettaz, P. Guilpain, C. Goulvestre, et al., "Radical Oxygen Species Production Induced by Advanced Oxidation Protein Products Predicts Clinical Evolution and Response to Treatment in Systemic Sclerosis," *Annals of the Rheumatic Diseases* 66, no. 9 (2007): 1202–1209.

42. A. K. Murray, T. L. Moore, J. B. Manning, et al., "Noninvasive Measurement of Skin Autofluorescence Is Increased in Patients With Systemic Sclerosis: An Indicator of Increased Advanced Glycation Endproducts?," *Journal of Rheumatology* 39, no. 8 (2012): 1654–1658.

43. V. Riccieri, A. Spadaro, L. Fuksa, O. Firuzi, L. Saso, and G. Valesini, "Specific Oxidative Stress Parameters Differently Correlate With Nailfold Capillaroscopy Changes and Organ Involvement in Systemic Sclerosis," *Clinical Rheumatology* 27, no. 2 (2008): 225–230.

44. S. Svegliati, T. Spadoni, G. Moroncini, and A. Gabrielli, "NADPH Oxidase, Oxidative Stress and Fibrosis in Systemic Sclerosis," *Free Radical Biology & Medicine* 125 (2018): 90–97.

45. R. Zhang, G. S. Kumar, U. Hansen, et al., "Oxidative Stress Promotes Fibrosis in Systemic Sclerosis Through Stabilization of a Kinase-Phosphatase Complex," *JCI Insight* 7, no. 8 (2022): 155761, https://doi.org/10.1172/jci.insight.155761.

46. A. Servettaz, C. Goulvestre, N. Kavian, et al., "Selective Oxidation of DNA Topoisomerase 1 Induces Systemic Sclerosis in the Mouse," *Journal of Immunology* 182, no. 9 (2009): 5855–5864, https://doi.org/10.4049/jimmunol.0803705.

Supporting Information

Additional supporting information can be found online in the Supporting Information section.